

In Silico screening of
Organo-selenium compounds 1

Radiation Processing of
Personal Protective Aprons 11

Enzymes driving
SARS-CoV-2 infection 19



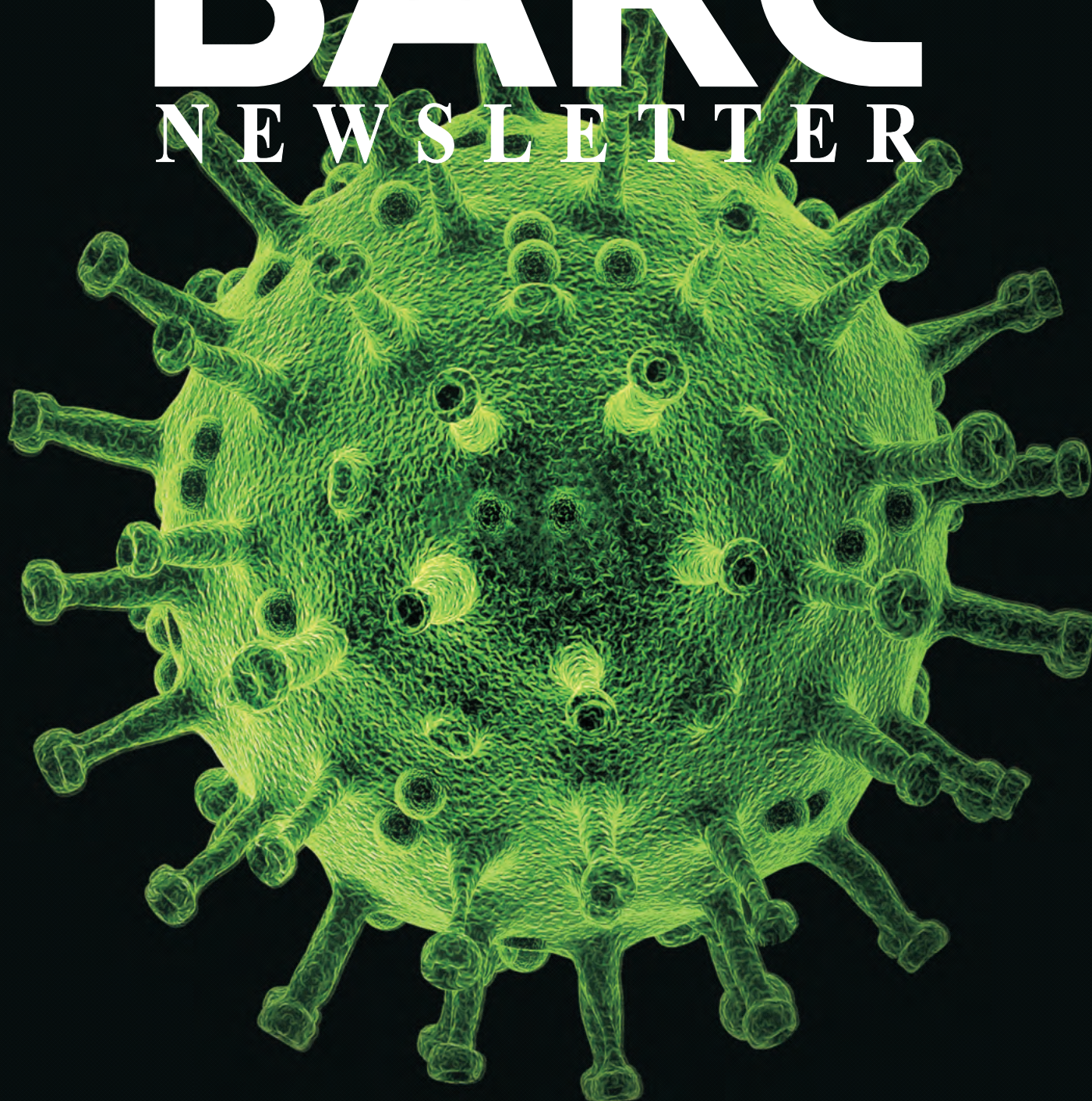
Bi-monthly • September - October • 2020

• Issue No. 368

ISSN: 0976-2108

BARC

NEWSLETTER



CONTENTS

Editorial Committee

Chairman

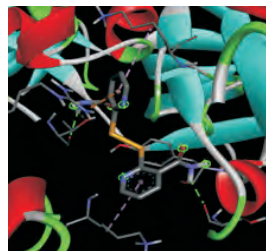
Dr. G.K. Dey
Materials Group

Editor

Dr. G. Ravi Kumar
SIRD

Members

Dr. A.K. Tyagi, Chemistry Divn.
Dr. S. Kannan, FCD
Dr. C.P. Kaushik, WMD
Dr. S. Mukhopadhyay,
Seismology Divn.
Dr. S.M. Yusuf, SSPD
Dr. B.K. Sapra, RP&AD
Dr. J.B. Singh, MMD
Dr. S.K. Sandur, RB&HSD
Dr. R. Mittal, SSPD
Dr. Smt. S. Mukhopadhyay, ChED



In Silico screening of Organo-selenium compounds for anti-viral activity against SARS-CoV2

B. G. Singh, A. Kunwar

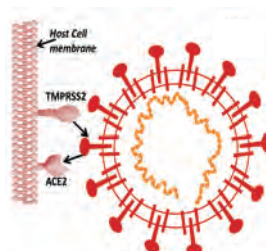
1

Radiation Processing of Personal Protective Aprons: A comprehensive analysis

K. A. Dubey, R. K. Mondal, R. K. Chaurasia, Usha Yadav, N. N. Bhat, Sarbani G. Laskar, J. P. Agarwal, Piyush Shrivastava, B. K. Sapra, Y. K. Bhardwaj



11



Enzymes driving SARS-CoV-2 infection: Key biological targets for therapy

Adish Tyagi and Sandeep Nigam

19

In Silico screening of Organo-selenium compounds for anti-viral activity against SARS-CoV2

B. G. Singh, A. Kunwar

Radiation & Photochemistry Division, Bhabha Atomic Research Centre, Mumbai - 400085
Homi Bhabha National Institute, Anushaktinagar, Mumbai - 400094

Abstract

Since the outbreak of the COVID-19 pandemic, researchers have been investigating several low molecular weight compounds, from both natural and synthetic origins, to design antiviral drugs against SARS-CoV-2. Recent work with selenium has demonstrated that its deficiency in human body leads to increased viral pathogenesis. Ebselen, a gold standard organoselenium compound, has shown promising anti-SARS-CoV-2 activity under *in-vitro* studies. With this background, the present study aimed to evaluate different organoselenium compounds and their sulfur analogues using a molecular docking approach to inhibit proteins that play a significant role in SARS-CoV-2 transmission. The organoselenium compounds used in the study are mostly synthesized *in-house*, including simple selenium containing amino acids and their derivatives, ebselen and their derivatives, selenopyridines and their derivatives. For the study, two viral protein Spike (S) Glycoprotein (PDB code: 6VXX) and Main Protease (3CLpro) (PDB code: 6LU7) of SARS-CoV-2 were used. The compounds were evaluated by comparing the docking scores calculated using AutoDock Vina as a docking engine. For comparison, standard drugs like Remdesivir and hydroxychloroquine (HOCQ) were used. The results showed that among all the molecules screened, the organoselenium compounds mostly showed stronger binding with the proteins as compared to their sulfur analogue, except oxidized glutathione. Additionally, ebselendiselenide (EbSeSeEb) and nicotinamide diselenide (NictSeSeNict) showed better inhibition to both the viral proteins as compared to Remdesivir and HOCQ. Thus, the present investigation highlights the influence of structure and substitution of organoselenium compound on their binding with the SARS-CoV-2 proteins and proposes NictSeSeNict as a candidate molecule for evaluating antiviral activity against SARS-CoV-2 using preclinical biological models.

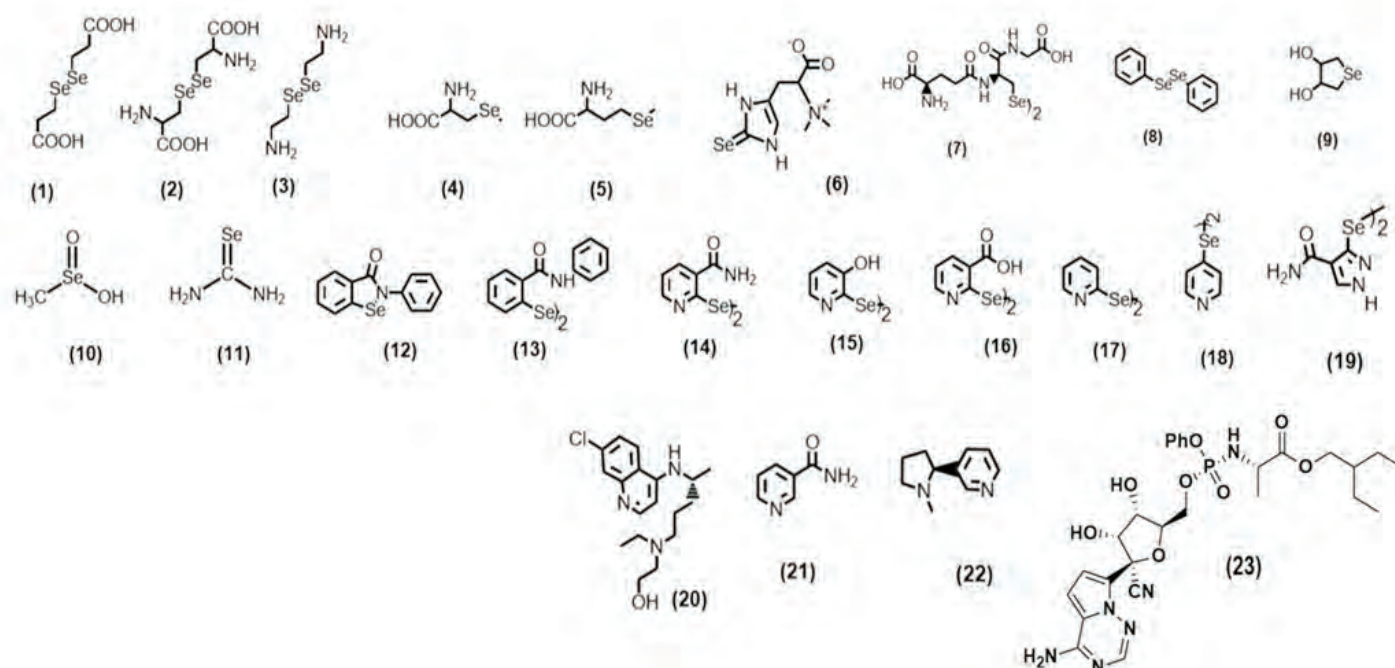
Introduction

Corona viruses (CoV) are a family of viruses containing positive strand ribonucleic acid (RNA) as a genetic material. In the past, these viruses have been reported for causing outbreaks of fetal pneumonia-like respiratory diseases in humans. The examples of such outbreaks are Severe Acute Respiratory Syndrome (SARS) and Middle East Respiratory Syndrome (MERS) during 2003 and 2012 respectively. Recently, in December 2019, several unidentified cases of pneumonia were reported from Wuhan, China. The molecular analysis of the bronchiolar lavage fluid (BAL) of these patients indicated the presence of a virus with RNA genome having more than 80% similarity with SARS-CoV. Accordingly, this virus was named as SARS-CoV-2 by International Virus

Classification Commission on February 11, 2020. In a very short period of time, this virus has spread to several countries and as of today, there are nearly 24.3 million confirmed cases of SARS-CoV-2 infections worldwide and more than 8,28,000 deaths. In view of the increasing infections, the World Health Organization (WHO) named the SARS-CoV2 induced pathology as COVID-19 and declared this outbreak a pandemic on March 12, 2020. Currently, there is no specific treatment available for COVID-19 and therefore the outbreak poses huge threat to humans [1].

With regard to developing a therapeutic drug against COVID-19, the best strategy is to identify an already approved drug with some other indication for the efficacy against COVID-19. The advantages of

using known drugs are that their dosages, route of administration, metabolic characteristics, potential efficacy and side effects are well characterized. This process is called drug repurposing and is the fastest way of drug development against new diseases. Indeed, several active clinical trials are in progress globally to evaluate several of food and drug administration (FDA) approved drugs for their efficacy against COVID-19. These include antiviral drugs, IL-6 antagonist and hydrochloroquine (HOCQ) among others. Although these treatment strategies have shown considerable success in the clinical setting, none of these have been approved by FDA as a standard treatment protocol for COVID-19. This warrants the need for the development of vaccine and/or new specific drugs against COVID-19 [1,2].



Scheme 1: Structure of organoselenium compounds screened for docking. In case of selenium compounds, their corresponding sulfur compounds and urea were also docked [Structure refers to 1. Diselenodipropanoic acid (DSePA), 2. Selenocystine (CysSeSeCys), 3. Selenocystamine (DSePAmine), 4. Methyl selenocysteine (MeSeCys), 5. Selenomethionine (SeM), 6. Selenoneine (SeHis), 7. Selenolutathioneoxi (GSeSeG), 8. Diphenyl diselenide (PhSeSePh), 9. Dihydroxyl selenolane (DHS), 10. Methane selenenic acid (MSeA), 11. Selenourea (SeU)*, 12. Ebselen (EbSe), 13. Ebselendiselenide (EbSeSeEb), 14. Nicotinamide diselenide (NictSeSeNict), 15. Pyridinoldiselenide (HOPySeSePyOH), 16. Nicotinic acid diselenide (CarPySeSePyCar), 17. 2-pyridine diselenide (2-PySeSePy), 18. 4-pyridine diselenide (4-PySeSePy), 19. Pyrazole amide diselenide (PyzSeSePyz), 20. Hydroxylchloroquine (HOCQ), 21. Nicotinamide, 22. Nicotine and 23. Remdesivir)

Results and Discussion

The genome of SARS-CoV2 encodes for structural proteins like spike (S) protein, envelope (E) protein, membrane (M) protein, nucleocapsid (N) protein and non-structural protein like replicase polyprotein. The structural proteins are involved in the formation of viral coat and the packaging of the RNA genome. The polyproteins undergo proteolytic cleavage to release proteins involved in viral replication and transcription by viral proteases 3CL^{pro} or M^{pro}, which by itself is released from polyproteins through autolytic cleavage. The S protein present in viral coat interacts with surface receptors like angiotensin-converting enzyme 2 (ACE2) to facilitate its entry in host cells (like lung epithelium). The functional importance of S and M^{pro} in establishing SARS-CoV2 infection along with the absence of a closely related homologue of these proteins in

humans, proposes them as an attractive target for the design of anti-viral drugs [8-11]. The molecular docking study of the above viral proteins with organoselenium compounds (Scheme 1) with varying functional groups have revealed a strong interaction with binding affinity ranging from approximately -3.0 kcal/mol to -9.0 kcal/mol. The binding energy of all the compounds with S and M^{pro} of SARS-CoV2 are listed in Table 1. The results of the docking studies with the individual proteins are discussed under following sections:

Interaction of organoselenium with S protein

The S protein, a homotrimeric glycoprotein, interacts with host receptor, ACE2, via the receptor-binding domain (RBD). The RBD is known to exist in at least two primary conformational states called the up (receptor-accessible) and down

(receptor-inaccessible) states. When the RBD is in the up state, the S protein is more “open” to facilitate the binding of ACE2. Studies have suggested that the down, receptor-inaccessible state, is more stable. This implies that low molecular weight molecules capable of binding RBD could stabilize the RBD in the down state, preventing the virus from interacting with ACE2; and thus limiting the COVID-19 infection [12]. Accordingly, for the present study, the down state form of the protein was used for docking (PDB code: 6VXX). The RBD region in S protein lies in the range from residues 331 to 524, while the most active amino acid residues are from 415 to 505 [13-16]. The binding energies of the organoselenium compound and their sulfur analogue with the S glycoprotein in terms of Vina scoring function are given in (Table 1). Docking results revealed that out of 19 selected organoselenium compounds,

Table 1: Binding energy of the organoselenium compounds, their sulfur analogues and reference molecules (Nicotine*, Nicotinamide* and Remdesivir*) with SARS-CoV2 proteins.

Sr. Nos	Compounds	Binding Energy (kcal/mol)			
		6VXX (S)		6LU7 (M ^{pro})	
		Se	S	Se	S
1	DSePA	-4.5	-4.1	-4.5	-3.9
2	CysSeSeCys	-5.5	-5.2	-4.7	-4.3
3	DSePAmine	-3.6	-3.5	-3.3	-3.1
4	MeSeCys	-4.2	-4.5	-4	-4.1
5	SeM	-4	-4	-3.4	-3.9
6	Se-His	-5.7	-5.8	-4.7	-4.7
7	GSeSeG	-6.6	-7.3	-5.1	-5.5
8	PhSeSePh	-5.8	-5.2	-5.2	-5
9	DHS	-4	-4	-3.8	-3.8
10	MSeA	-3.8	-3	-3.1	-3.1
11	SeU	-3.1	-3.6	-3.2	-3.3
12	EbSe	-6.3	-6.3	-5.4	-5.4
13	EbSeSeEb	-9.4	8	-7	-6.2
14	NictSeSeNict	-8.1	-7.4	-6.6	-5.7
15	HOPySeSePyOH	-6.8	-6	-5.8	-5
16	CarPySeSePyCar	-7.1	-6.4	-5.8	-5.2
17	2-PySeSePy	-6.1	-5.6	-5.1	-4.8
18	4-PySeSePy	-5.3	-5.4	-4.5	-4.2
19	PyzSeSePyz	-8	-7.5	-6.2	-5.5
20	Nicotinamide*	-5		-4.3	
21	Nicotine*	-5.2		-4.2	
22	HOCQ*	-6.3		-4.9	
23	Remdesivir*	-8.2		-3.2	

the aliphatic selenium compounds showed lower binding as compared to the aromatic derivatives. In this series of compounds, only EbSeSeEb and NictSeSeNict showed higher binding interaction compared to the standard molecule, HOCQ and Remdesivir. The carboxylate group in DSePA, an aliphatic diselenide, is involved in conventional hydrogen bonding with Arg408, Gln 409 and Lys 417, while the aliphatic and diselenide moiety are involved in Van der Waals interaction with the amino acid residue (Table 2). Further in CysSeSeCys, where an amino group is added as compared to DSePA, along with the hydrogen bonding (Tyr369, Ser383, Thr415, Gln414, Arg408, Pro384, Ser383),

alkyl interaction of Lys375 and Cys379 with the diselenide bond is observed. The amino group of CysSeSeCys is found to be involved in hydrogen bonding with Thr415, an amino acid involved in the receptor binding domain of S protein. This results in an increase in the binding energy of CysSeSeCys as compared to DSePA (Interaction as depicted in Table 2). On increasing the peptide bond as seen in GSeSeG and GSSG, the number of conventional bonds increase, which is reflected in the increase in the binding energy of these compounds with the S-protein. Also, the number of interactions observed is more in case of GSSG as compared to GSeSeG, which may be attributed to

the size of the molecule to fit in the binding site. This results in the higher binding energy of GSSG. The aromatic organoselenium compounds showed higher binding energy compared to the similar molecular weight aliphatic analogues (for eg DSePA). This is attributed to the induction of pi-alkyl interaction along with the conventional hydrogen bonding interaction. Further, comparing the binding energy of aromatic compounds with different functional group such as carboxylate (CarPySeSePyCar), hydroxy (HOPySeSePyOH) and amide (NictSeSeNict), indicated that the compounds with amide functional group showed higher binding with the

Table 2: The amino acid residues involved in binding of organoselenium compounds with viral S protein (PDB Code: 6VXX). ●●●●● represent hydrogen bonding, Van der Waals binding, pi-alkyl interaction, pi-cation attraction interaction and repulsive interaction.

		2D Interaction
1.	DSePA Binding Energy = -4.5kcal/mol	
2.	CysSeSeCys Binding Energy = -5.5kcal/mol	
3	GSeSeG Binding Energy = - 6.6kcal/mol	
4	GSSG Binding Energy = - 7.3 kcal/mol	

5	<p>NictSeSeNict Binding Energy= -8.1kcal/mol</p>	
6	<p>Ebselen Binding Energy = -6.3 kcal/mol</p>	
7	<p>Ebselendiselenide Binding Energy = -9.4 kcal/mol</p>	
8	<p>HOCQ Binding energy = -6.3 kcal/mol</p>	
9	<p>Remdesivir Binding energy = -8.2 kcal/mol</p>	

protein. The increase in binding energy may be attributed to the presence of hydrogen bond between -NH atom of amide and Thr415 of the protein. The amino acid, Thr415, is involved in the receptor binding domain of the S-protein. Similarly, the influence of heterocyclic diselenide can be compared from the values obtained for EbSeSeEb, PyzSeSePyz and NictSeSeNict. The presence of the N-hetrocyclic ring is found to influence the binding of the compound slightly away from the Thr415 residue where as the simple aromatic ring as seen in ebselen and its diselenide binds to Thr415, thus increasing the binding with the S-protein. Further, the plain ligand without selenium moiety was

also docked to evaluate the influence of selenium atom in the binding. It was observed that the binding energy of the nictotiamide ligand was lesser compared to the diselenide form. The binding energy of 2,2'-dipyrdine diselenide was higher than the nicotinamide ligand. Higher binding values may be due to the presence of two aromatic rings in the molecule. The docking of the selone (the monoselenide form) form of NictSeSeNict showed similar value to nicotinamide ligand. The dipyrndine with amide group at the ortho position may itself be showing good affinity for S-protein. However, this molecule is not easy to synthesize and is also expected to be instable. On the

contrary, the diselenide bond may act as a bridge to form the dinicotinamide moiety to get the desired activity.

Interaction of organoselenium with M^{pro} protein

M^{pro} protein is a homodimer comprising of three domains viz., domain I (residue 8-101), domain II (residue 102-184) and domain III (residue 201-203) and a long loop (residues 201–303). The catalytic region is formed by the dyad His41-Cys145 that is highly conserved among the coronavirus proteases. This probable binding site for substrates is located in a cleft region between domains I and II, which is similar to that observed in the trypsin-like serine proteases. Table 3 shows the nature of

Table 3: The amino acid residues involved in binding of the organoselenium compounds and the viral M^{pro} protein (PDB Code: 6LU7). ●●●●● represent hydrogen bonding, Van der Waals binding, pi-alkyl interaction, pi-cation attraction interaction and repulsive interaction.

		2D Interaction
1	DSePA Binding energy: -4.5 kcal/mol	
2	CysSeSeCys Binding energy = -4.7 kcal/mol	
3	GSeSeG Binding energy = -5.1 kcal/mol	

the binding interactions of some of the in-house synthesized organoselenium compounds like DSePA and NictSeSeNict along with the standard compounds like CysSeSeCys, ebselen, HOCQ and Remdesivir with SARS-CoV-2 main protease. The binding energy of DSePA is found to be lower than the other organoselenium compounds but it is still higher than the standard molecules, HOCQ and Remdesivir. The carboxylate group of DSePA is involved in the hydrogen bonding with Gly23, Cys22, Asn45, Thr24, Thr25, while the aliphatic alkyl diselenide chain is involved in Van der Waals interaction. However, it binds only in the domain I and is slightly away from the active site. In CySeSeCys, the amino acid residue Asp48, Ile43, Lys61, Cys44, Cys22 and Thr25 are involved in hydrogen bonding with the amino and carboxylate group of the diselenide. There is an unfavorable binding with Thr24 and the carboxylate group. Like DSePA, CysSeSeCys also binds with the amino acid in the extreme right side of domain I, these factors may be responsible for the low binding of CysSeSeCys with Mpro. As seen from the interaction in Table 3, docking of Mpro with GSeSeG, which has more number of amide bonds, exhibited higher binding energy. In case of GSSG, along with the conventional hydrogen bonding, an additional pi-alkyl interaction exists with Cys845, which is at the interface between domain I and II. This may be responsible for the higher binding energy of GSSG as compared to GSeSeG. The binding of PhSeSePh is also higher compared to similar molecular weight aliphatic compound DSePA. The lower binding energy of the aliphatic compound may be due to the wobbling of the alkyl chain, which is otherwise rigid in case of aromatic compound. Similarly, Ebselen shows binding with the amino acids present

in the domain I but slightly towards the end of domain I. Hence its binding energy is also low. In case of NictSeSeNict and EbSeSeEb, it can be seen that these compounds effectively bind at the interface and near the catalytic site. The amide functional group in these molecules are involved in hydrogen bonding with polar amino residues, but the presence of aromatic ring increases the interaction between the selenium compounds and the protease by induction of hydrophobic and pi-alkyl interactions. Additionally, the binding energy of the selenium compounds is found to be higher as compared with their analogous sulfur compounds. This is attributed to the higher contribution of the Van der Waals interaction in selenium compounds, which arises due to its higher polarizability.

Conclusions & Future Directions

The present investigation revealed that organoselenium compounds exhibited higher binding affinity to the SARS-CoV2 proteins and can be suitable candidate molecules for designing an antiviral drug. Among the library of 22 organoselenium compounds studied in the present work, NictSeSeNict and EbSeSeEb showed the highest affinity for two viral proteins, namely S and M^{pro}. The molecular examination of the binding interaction of structurally related compounds with varying functional groups indicated that aromatic ring coupled with amide group plays an important role in establishing the interaction of organoselenium compound with the viral proteins. These results are only preliminary and our future studies will be focused to evaluate the most potent compound like NictSeSeNict by using recombinant viral proteins and active viruses. Additionally, DSePA, reported for its anti-inflammatory activity in lungs also exhibited a moderate interaction with the viral proteins, and therefore may also be effective in

suppressing or delaying the pneumonia associated with COVID19. However, this hypothesis needs to be rigorously tested using preclinical models.

Acknowledgement

Authors thank Dr. Awadhesh Kumar, HOD, RPCD and Dr. A. K. Tyagi, Associate Director, Chemistry Group, for the support and encouragement during the course of study.

Corresponding author & email:

B. G. Singh (beenam@barc.gov.in)

References

1. C. Liu, Q. Zhou, Y. Li, L. V. Garner, S. P. Watkins, L. J. Carter, J. Smoot, A. C. Gregg, A. D. Daniels, S. Jervey, D. Albaiu, ACS Cent Sci. 2020, 6, 315–331
2. H. Amawi, G. A. Deiab, A. A. Aljabali, K. Dua, M. M. Tambuwala, Ther. Deliv. 2020 Apr; (doi: 10.4155/tde-2020-0035).
3. L. Sancineto, A. Mariotti, L. Bagnoli, F. Marini, J. Desantis, N. Iraci, C. Santi, C. Pannecouque, O. Tabarrini, J. Med. Chem. 2015, 58, 9601–9614
4. P. K. Sahu, T. Umme, J. Yu, A. Nayak, G. Kim, M. Noh, J. Y. Lee, D. D. Kim, L. S. Jeong, J. Med. Chem. 2015, 58, 21, 8734–8738
5. Z. Jin, X. Du, Y. Xu, Y. Deng, M. Liu, Y. Zhao, B. Zhang, X. Li, L. Zhang, C. Peng, Y. Duan, J. Yu, L. Wang, K. Yang, F. Liu, R. Jiang, X. Yang, T. You, X. Liu, X. Yang, F. Bai, H. Liu, X. Liu, L. W. Guddat, W. Xu, G. Xiao, C. Qin, Z. Shi, H. Jiang, Z. Rao, H. Yang, Nature, 2020, 582, 202–204, <https://doi.org/10.1038/s41586-020-2223-y>
6. K. A. Gandhi, J. S. Goda, V. V. Gandhi, A. Sadanpurwaia, V. K. Jain, K. Joshi, S. Epari, S. Rane, B. Mohanty, P. Chaudhary, S. Kumbhavi, A. Kunwar, V. Gota, K.

- I. Priyadarsini, *Free Radic. Biol. Med.* 2019, 145, 8-19.
7. D. Maurya, D. Sharma C, *ChemRxiv*, 2020, doi: 10.26434/chemrxiv.12110214
8. W. Tai, L. He, X. Zhang, J. Pu, D. Voronin, S. Jiang, Y. Zhou, L. D, *Cell. Mol. Immuno.* 2020, 17, 613–620.
9. J. Shang, G. Ye, K. Shi, Y. Wan, C. Luo, H. Aihara, Q. Geng, A. Auerbach, F. Li, *Nature*, 2020, 581, 221–224.
10. C. Yi, X. Sun, J. Ye, L. Ding, M. Liu, Z. Yang, X. Lu, Y. Zhang, L. Ma, W. Gu, A. Qu, J. Xu, Z. Shi, Z. Ling, B. Sun, *Cell. Mol. Immuno.* 2020, 17, 621–630.
11. J. Shanga, Y. Wana, C. Luo, G. Yea, Q. Genga, A. Auerbach, F. Lia, *Proc. Natl. Acad. Sci. U.S.A.*, 2020, 117, 11727–11734.
12. L. Zhanj, D. Lin, X. Sun, U. Curth, C. Drosten, L. Sauerhering, S. Becker, K. Rox, R. Hilgenfeld, *Science*, 2020, 368, 409–412.
13. P. Calligar, S. Bobone, G. Ricci, A. Bocedi, *Viruses* 2020, 12, 445-458.
14. J. S. Morse, T. Lalonde, S. Xu, W. Li, *ChemRxiv*, 2020, doi.org/10.26434/chemrxiv11728983.v1
15. Lisheng Wang, Yiru Wang, Dawei Ye, Qingquan Liu, *Int. J. Antimicrob. Agents*, <https://doi.org/10.1016/j.ijantimicag.2020.105948>
16. M. Macchiagodena, M. Pagliai, P. Procacci, *Chem. Phys. Lett.* 2020, 750, 137489 - 137494

Radiation Processing of Personal Protective Aprons: A comprehensive analysis

**K. A. Dubey, R. K. Mondal, R. K. Chaurasia, Usha Yadav, N. N. Bhat,
B. K. Sapra, Y. K. Bhardwaj**

Bhabha Atomic Research Centre, Trombay, Mumbai-400085

Sarbani G. Laskar, J. P. Agarwal

Tata Memorial Centre, Parel, Mumbai-400012

Piyush Shrivastava

Board of Radiation & Isotope Technology, Vashi, Navi Mumbai-400703

Abstract

Personal protective equipments (PPE) play a key role in the fight against COVID-19 pandemic. Aprons, a major constituent of PPE, are designed for single-time use. COVID-19 may create a temporary, but huge setback in normal demand-supply of PPE aprons. A possible solution would be the sterilization of the PPEs for reuse. It is well known that high energy radiation has high efficacy for killing pathogens. Unlike UV radiation, gamma rays penetrate deeper into matter. Its effect on family of corona viruses is also well proven. However, the possible adverse effects of irradiation on PPE aprons has not yet been reported. The article reports extensive work carried out to develop a radiation processing protocol that assures desired Sterility Assurance Level (SAL) while maintaining acceptable physicochemical properties in radiation-processed indigenously manufactured PPE aprons. The aprons were evaluated for their mechanical properties, blood penetration resistance and morphological characteristics. Finally, protocols for radiation processing of PPEs, performance evaluation and their use in the real setting were developed and submitted to the Union Ministry of Health & Family Welfare.

Introduction

The COVID-19 pandemic may result in a short supply of single personal protective equipment (PPE) on account of demand-supply imbalance [1]. As aprons are among the major components of PPE, demand for them is expected to rise. Thus, globally there has been an impetus to investigate the reusability of PPE post adequate sterilization [2]. Two major considerations for re-use of these PPE aprons are: i) the sterilization method should effectively kill pathogens ii) the functional requirement is fulfilled after sterilization. Plasma gas sterilization, vaporized H₂O₂ sterilization, dry heat sterilization, chemical sterilization, steam sterilization and radiation sterilization are the major sterilization methods for treating medical products. Among them, radiation sterilization has its distinct advantage as it is carried out at room temperature with the possibility

of sterilization in sealed units. A dose of 25 kGy is recommended for sterilization of medical products. Gamma radiation-induced inactivation of viruses of the SARS-COV family has been extensively documented [4]. The sterilization dose for the virus is a function of initial viral load, D10 value, and the type of virus. It has been recently reported that gamma radiation dose of 10 kGy is sufficient to reduce titers by 4-5 log₁₀ and a dose of 20 kGy is sufficient for complete inactivation of the virus. Further, they suggest a dose of 30 kGy is sufficient to inactivate MERS-CoV in most laboratory cell cultures or tissue-based assays [5]. The same has been validated by studies of Hume et al. on RNA-viruses with a reported dose of 30 kGy for achieving sterility assurance level (SAL) of 10⁻⁶ [6]. However, there is no report available on the possible adverse impact of high energy radiation on the mechanical integrity and performance of PPE

aprons and its fabric. This report presents a systematic study on effects of radiation on physico-chemical properties and performances of PPE aprons and the development of a protocol for radiation processing of used PPEs.

Methodology

For experimental studies, 6 x 6 inch sized units were cut from aprons and irradiated in the gamma chamber (GC-5000) under a dose rate of 6.2 kGy/hour as determined by Fricke dosimetry. All samples were packed in polyethylene (PE) bags and irradiated at a dose rate of 3.1 kGy/hour using a lead attenuator. For large scale irradiation, the aprons were packed in cardboard cartons and the cartons were placed in Tote boxes for irradiation with proper dose indicator displayed on the walls of cartons. The irradiated aprons were initially evaluated manually and later a piece of size 6" x 6" was cut from the apron and

evaluated for mechanical properties using Universal Testing Machine (UTS), equipped with a load cell of 100 N at a head speed of 20mm/min. Fourier transform infrared spectroscopy (FTIR) from Bruker in Attenuated Total Reflection (ATR) mode and Rigaku XRD diffractometer were used for material characterization. Synthetic blood penetration resistance test was carried

out using an in-house developed set-up confirming to the guidelines of ISO 16603, ASTM F1670 and JIST 8060 and 8122. The apron fabric was tested in the applied fluid pressure range of 40-300 mmHg. Morphological changes in the apron fabric were observed through microscopic observations. Table 1 gives the details of the aprons investigated.

Table 1: PPE source & designated code

Make	Sample code
Prime Wear Hygiene (India), Pvt. Ltd. Thane -1	A
Not mentioned	B
Tyvek-400	C
Not mentioned	D
Not mentioned	E
Not mentioned	F
Prime Wear Hygiene (India) Pvt. Ltd, Thane-2	G
Fasten Medical Solutions, Cochin	H
Aditya Birla Fashion & Retail Ltd., Bangalore	J
Shahi Exports Pvt. Ltd., Bangalore	K
Aditya Life Science, Ahmedabad	L
Hanshil Enterprise, Rajkot	M
Pioneer Hygiene products	N

Laboratory scale studies

The samples were designated as A, B, and C and irradiated in the gamma chamber for different doses and their mechanical properties were evaluated. All samples showed a systematic decrease in mechanical properties on irradiation. The apron sample C (Tyvek brand) showed minimum decrease while “A” showed maximum decrease in mechanical properties. Figure 1 shows the results of these studies. Based on these studies and as per the values reported in the literature, aprons of PPE sets were consequently irradiated to a dose of ~30 kGy at radiation processing plant (RPP), Vashi, and were later evaluated.

Processing of aprons on a larger scale

The radiation processed aprons were initially subjected to manual evaluation. They were examined for any visible change in color, deterioration in mechanical properties (by physical push-pull), and for any pungent smell. No noticeable color change or pungent smell was observed in any of the aprons. Test samples G and H failed push-pull test. Therefore, unirradiated G and H were also subjected to pull-push test and both of them failed. The response of other irradiated samples to push-pull was

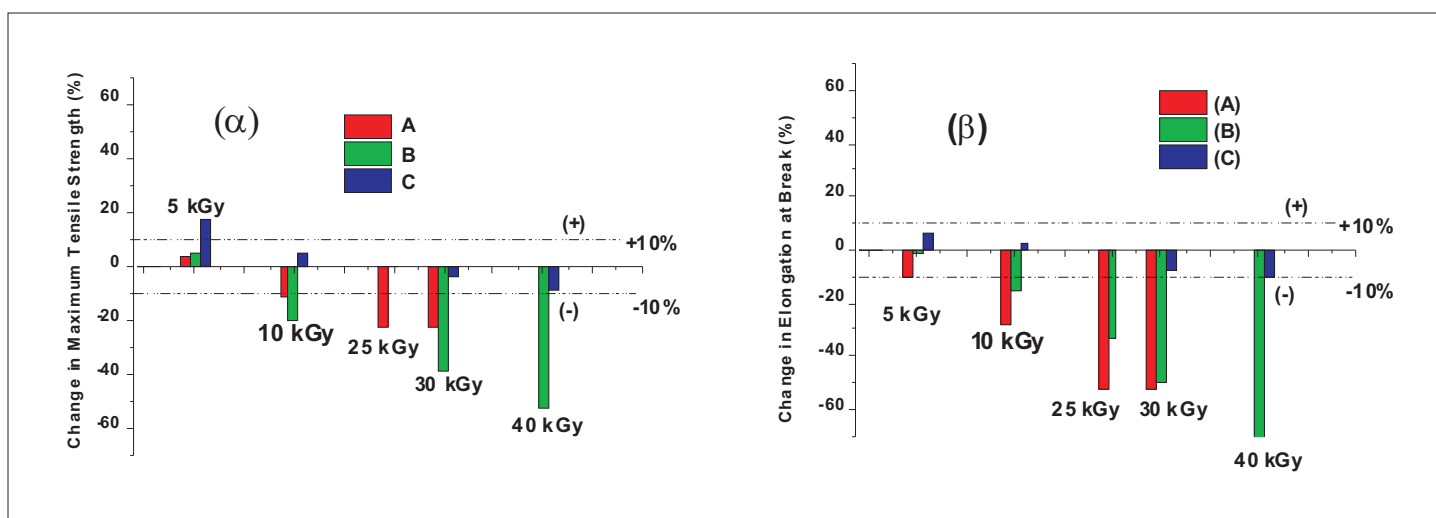


Fig. 1: (α) %Change in maximum tensile strength (β)% Change in elongation at break



Fig. 2: Manual evaluation of Aprons

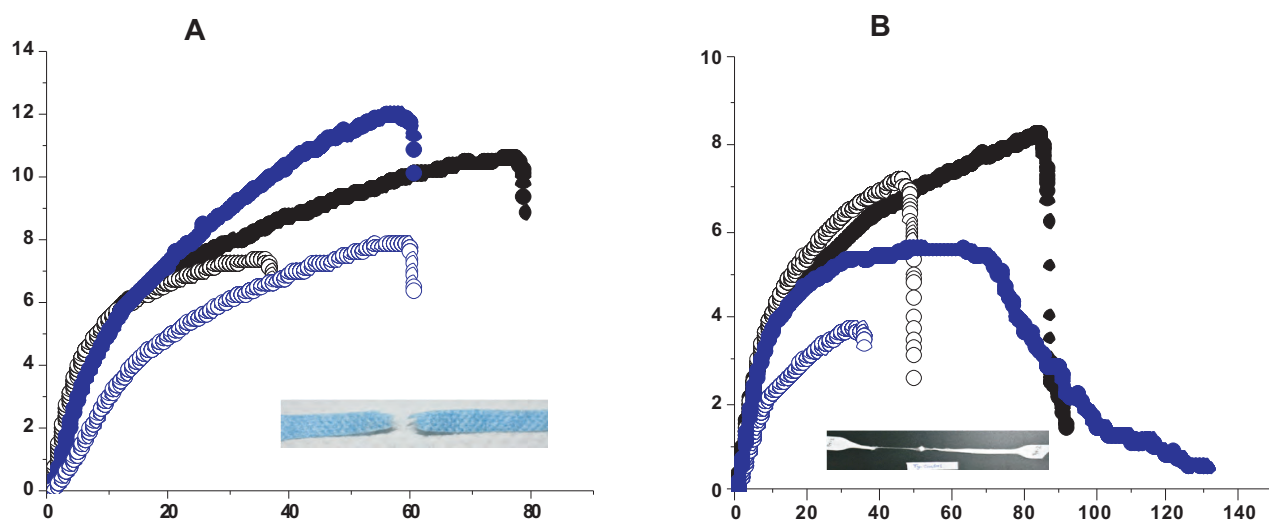


Fig. 3: Stress-Strain profiles for two types of failures (A) Abrupt failure (B) Delayed failure

positive as none of them showed mechanical failure when tested in multiple directions.

The elasticity of the rubbery rubber band at limb ends, the strength of samples at the seam and elasticity of hood lining were also found to be intact, after irradiation. Figure 2 shows pictures of the manual evaluation of aprons. Similar to the laboratory scale studies the aprons after irradiation were evaluated for their mechanical properties. Figure 3 gives representative stress-strain

profiles of some of the samples. Mainly, two types of stress-strain profiles were observed. For some samples, the tensile profiles showed an initial elastic region followed by plastic region and then abrupt failure while for others the plastic region was followed by a failure region where the sample slowly deteriorated to failure {Figure 3(B)}. Table 2 shows the results of these studies. It is clear from the table that for all the samples there was a decrease in tensile strength & elongation-at-break (EB) on irradiation though, to different

extents. The decrease in mechanical properties to different extents indicated that the aprons were either made of different materials or by different fabrication processes. To the best of our knowledge, no benchmark value for the mechanical properties of PPE aprons has been reported in the literature. Though there is a decrease in mechanical properties for aprons after irradiation, still the data in Table 2 clearly indicates that they are strong enough for reuse. Based on these studies, for a source strength of 680kCi and for an absorbed dose of 30

Table 2: Mechanical properties of aprons

Sample	Tensile strength (MPa)		Elongation at break (%)	
	Unirradiated	Irradiated (30 kGy)	Unirradiated	Irradiated (30 kGy)
D	11.61±1.22	7.43±0.44	63.1±9.21	31.32±1.32
E	12.48±1.01	5.68±0.32	97.82±4.21	18.71±3.72
F	5.12±0.56	3.61±0.25	49.94±14.41	35.41±0.61
G	9.34±0.09	6.66±0.44	48.82±2.04	21.47±1.63
H	8.96±0.23	6.69±0.22	97.45±9.97	46.22±1.58
J	10.01±1.66	7.64±0.51	78.74±21.67	37.34±4.23
K	8.73±0.38	6.58±0.81	80.67±7.67	42.33±7.53
L	8.09±0.01	4.63±0.14	80.27±0.01	43.05±3.31
M	-----	7.82±0.26	-----	33.91±1.43
N	-----	8.62±0.72	-----	83.62±12.12

kGy dose, it was estimated that 3500 aprons can be processed within a duration of 14 hours in RPP Vashi.

Spectroscopic and XRD analysis

Mechanical analysis of aprons indicated that they may be made of different polymers. Therefore, the FTIR analysis of apron material was carried out to ascertain their constituent polymer. The samples which showed delayed failure were analyzed for both the faces. Figure 4 shows representative ATR-FTIR spectra of some of the samples.

None of the samples tested were observed to be made of two different constituent polymers on its two faces. The vibrational modes observed in the FTIR spectra indicated that most of the aprons were predominantly made either of polypropylene or polyethylene and also polypropylene

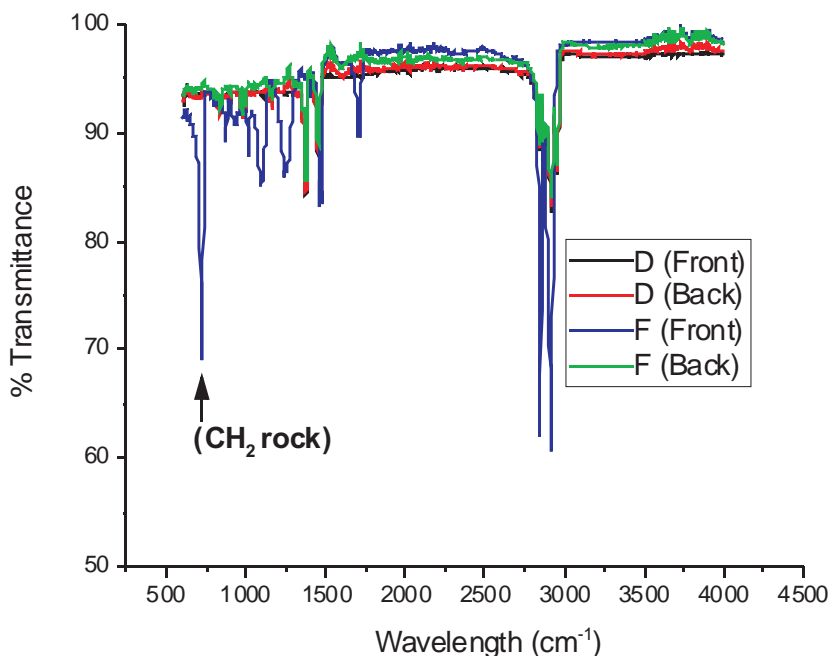


Fig. 4: Representative ATR-FTIR spectra

Table 3: Spectroscopic and XRD identification of apron material

Sample	Major fraction of polymer (ATR-FTIR)	Major fraction of polymer (XRD)
A	PP	PP
B	PP	PP
C	PE	PE
D	PP	PP
E	PP	PP
F	PE	PE
G	PP	PP
H	PP	PP
J	PP	PP
K	PP-PE blend	PP-PE blend
L	PE	PE
M	PP	PP
N	PE	PE

blended with polyethylene in one instance (Table 3). This observation was further supported by the XRD analysis of samples (Figure 5).

Synthetic blood penetration resistance (SBPR) test

The results of the test with respect to the sustained pressure on apron fabrics before and after irradiation are shown in Table 4. On correlating the data in table 3 & 4, it may be concluded that synthetic blood penetration resistance of the apron fabric is not material specific. It seems it also depends on the process used for making the apron cloth.

Morphological changes in apron fabric

Morphological changes in the apron fabric were observed through microscopic observations. Microscopic image of one of the

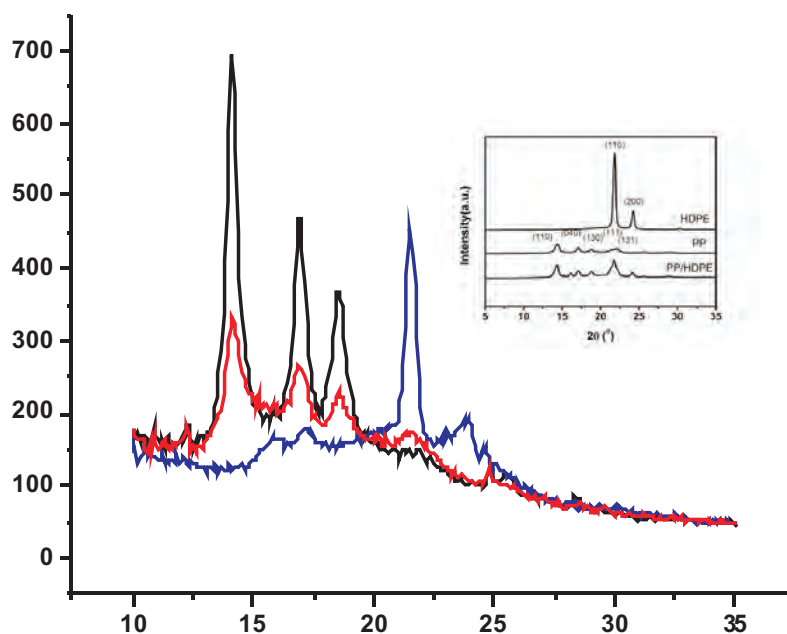


Fig. 5: XRD patterns of samples

Table 4: Blood penetration test

Sample	Tolerance pressure (mm Hg)		JIST8122 classification	Performance of material
	Unirradiated	Irradiated (30 kGy)		
D	<40	<40	Class-1	Low
E	<40	<40	Class-1	Low
F	<40	<40	Class-1	Low
J	>300	>300	Class-6	High
K	>300	>300	Class-6	High
L	>300	>300	Class-6	High

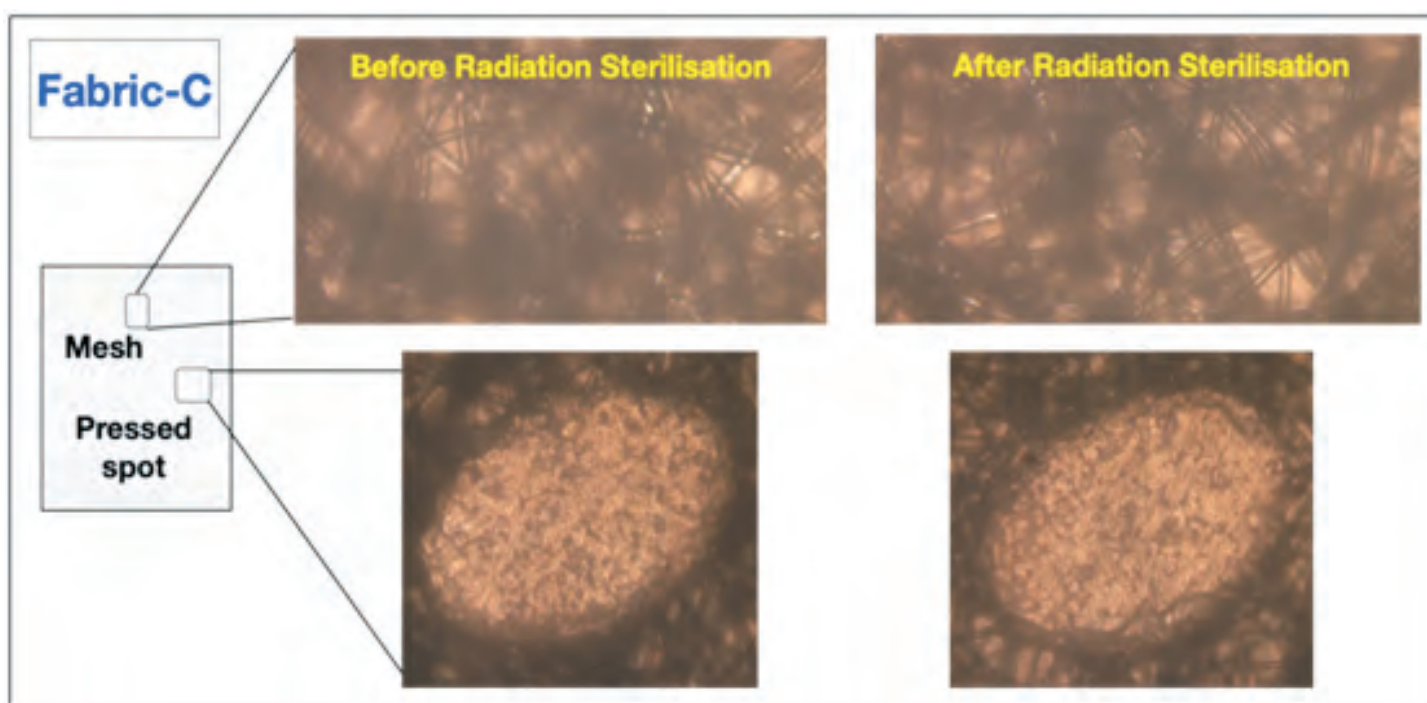


Fig. 6: Microscopic (bright field) image of sample F (Magnification 100 X)

representative sample (sample F) is shown in Figure 6. No observable change in number and size of voids was observed in the pressed or mesh region. For other samples too similar observations were made. Morphological observations were in sync with the SBPR test observations for all samples, where no change in tolerance pressure was observed post irradiation.

Conclusion

Radiation processing is an effective process for enabling the reuse of PPE aprons. Based on the positive outcomes of these investigations, a Standard Operating Procedure (SOP) for radiation processing of used PPE aprons has been prepared and submitted to the Union Ministry of Health & Family Welfare.

Corresponding author and email:

Y . K . B h a r d w a j
(ykbhard@barc.gov.in)

Acknowledgment

The authors sincerely thank Shri K. N. Vyas, Chairman AEC and Secretary DAE, Dr. A. K. Mohanty, Director, BARC, Dr. R. A. Badwe, Director, Tata Memorial Centre, Dr. P. K. Pujari, Director Radiochemistry & Isotope

Group, BARC, Shri R. M. Suresh Babu, Associate Director, Health, Safety and Environment Group, Dr. C. S. Pramesh, TMC and Dr. Pankaj Chaturvedi, TMH for their constant encouragement and keen interest in this work.

References

1. S. Feng, C. Shen, N. Xia, W. Song, M. Fan, and B. J. Cowling. *Lancet Respir Med.*(2020) 8(5) 434-436.
2. World Health Organization article on Rational Use of Personal Protective Equipment for Coronavirus Disease (COVID-19) and considerations during severe shortages; Interim guidance, 6 April 2020.
3. R. Sullivan, A. C. Fassolitis, E. P. Larkin, R. B.. Read, Jr.andJ. T. Peeler. *Appl Microbiol.*; (1971) 22(1) 61-65.
4. F. Feldmann, W. L. Shupert, E. Haddock, B. Twardoski and H. Feldmann. *Am J Trop Med Hyg.*; (2019) 100 1275-1277.
5. M. Kumar, S. Mazur, B. L. Ork, E. Postnikova, L. E. Hensley, P. B. Jahrling, R. Johnson and M. R. Holbrook.J. *Viol. Methods.*; (2015) 223 13-18.
6. A. J. Hume, J. Ames, L. J. Rennick, W. P. Duprex, A.Marzi, J. Tonkiss, E. Mühlberger, *Viruses* (2016) 8(7) 204-215.

Enzymes driving SARS-CoV-2 infection: Key biological targets for therapy

Adish Tyagi and Sandeep Nigam

Chemistry Division

Bhabha Atomic Research Centre, Trombay, Mumbai-400085

Abstract

The SARS-CoV-2 virus is responsible for the global COVID-19 pandemic. Specific treatment or vaccine for cure against SARS-CoV-2 infection is yet to be released. It is widely understood that various enzymes present in the human body assist the growth of SARS-CoV-2. These enzymes play a pivotal role in mediating the virus' entry and replication which makes them an attractive biological target for therapeutic purposes. Analyzing the structure, binding region, catalytic site of these enzymes may help to identify high-throughput inhibitor candidates, which may help curtail the virus' life cycle and also arrest the infection. This review summarizes the role of enzymes in catalyzing cell infection by under SARS-CoV-2, and promising drugs aiming these enzymes for inhibition.

Introduction

Zoonotic viruses pose a serious threat to public health [1]. Belonging to this family of deadly viruses, SARS-CoV-2, is responsible for COVID-19, an infectious respiratory disease which has emerged into a global pandemic claiming millions of lives within a short span of two months [2-4]. SARS-CoV-2 has 86%, 50% and 96% similarity to the genome of the

severely acute respiratory syndrome virus (SARS-CoV), the middle-east respiratory syndrome virus (MERS-CoV) and the horseshoe bat coronavirus RTG13, respectively [2]. The SARS-CoV-2 is a beta-coronavirus belonging to the family of Coronaviridae [5]. It consists of ~30,000 single stranded RNA nucleotides packaged inside the nucleocapsid protein (N) which are further wrapped inside the membrane

protein (M), spike protein (S) and envelop protein (E) (Figure-1). The SARS-CoV-2 viral genome encodes for 29 proteins, out of which 16 are non-structural proteins (nsp), which aid virus' replication and infection, 4 of them are structural proteins (S, E, M, N) responsible for virus architecture and the rest are accessory proteins for countering the host immune response [6].

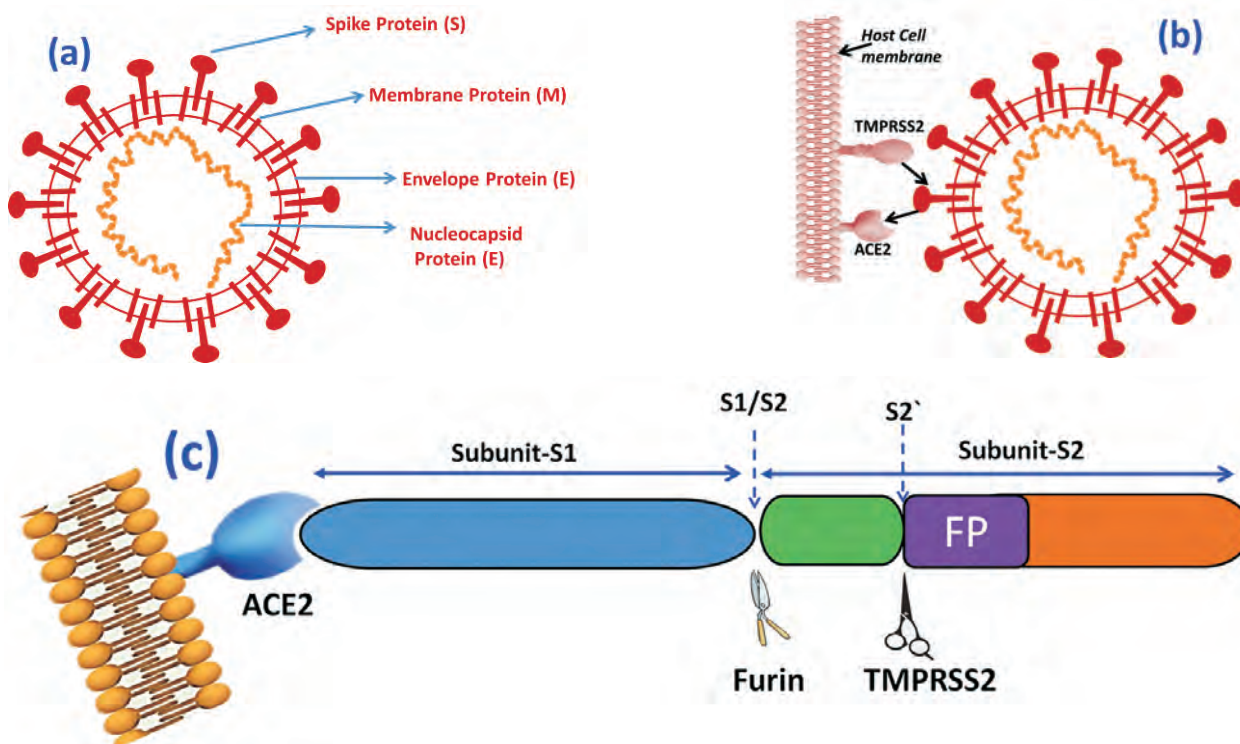


Fig. 1: (a) Structure of SARS-CoV-2. (b) Enzymes of host cell facilitating entry of virus in the cell. (c) (Cartoon representation of spike protein interaction) Interaction of spike protein with host cell enzymes (ACE2, Furin, TMPRSS2) to facilitate virus entry in human cell

The SARS-CoV-2 infection starts as soon as the virus enters the host/human cell. The spike (S) protein of the virus binds to angiotensin converting receptor enzyme 2 (ACE2), which is present on the surface of host cell and initiates fusion of its membrane with the cell membrane with the help of another host enzyme called transmembrane serine protease 2 (TRMPSS2) [7-8] (Figure-1). The ACE2 receptor is an immunomodulator which regulates the blood pressure, and is present in plenty in the cells of lungs, heart, kidneys etc. After entering host cell, the SARS-CoV-2 genomic RNA is released into the cytoplasm of the cell. The entire ~ 30,000 single stranded RNA nucleotides is translated by the host cell ribosomes. The translation products are called as polyprotein 1a (pp1a) and polyprotein 1ab (pp1ab), both having an overlapped

polypeptide chain structure(Figure-2). These polypeptide chains contain multiple, distinct non-structural proteins (nsp 1–16), which regulate replication of viral RNA and assembly of newly generated copies and their maturation. However, the polypeptide needs to be cut into small functional proteins to carry out the replication and virion assembly. The enzymes, papain-like protease (PL_{pro}) and chymotrypsin like protease (3CL_{pro}) or main protease (M_{pro}), cuts these polyproteins to yield 16 small functional proteins (16 nsps). The role of each nsp is well defined. For example, the RNA-dependent RNA polymerase enzyme is encoded in nsp12 [9] which assist in RNA synthesis, genome and subgenomic RNA. Researchers are considering a number of potential drugs molecules which can bind to these key enzymes and inhibit their functioning and

subsequently arrest the infection. However, this requires knowledge about enzyme structure, binding region, catalytic site, etc. In the following sections, the enzymes playing key role in SARS-CoV2 infections are discussed in detail.

Host cell enzyme and entry of virus in the cell

Coronaviruses are named for the crown of protein spikes covering their outer membrane surface. All coronaviruses, including SARS-CoV-2, use the spike proteins (S) for binding with the host cell receptor for cell entry. The spike protein is a homotrimeric glycoprotein where each monomer is divided into S1 and S2 sub-units as shown in Figure 1 [10]. S1 sub-unit owns the domain for host cell attachment called receptor binding domain (RBD), which is a binding site with host cell receptor ACE2. On the other hand, S2 sub-unit contains fusion peptides responsible for fusion of virus membrane with the host cell membrane [10]. However, ensuing to virus-host cell binding (S1-hACE2), the fusion process of virus and host cell membrane cannot occur until and unless S protein is cleaved at S1/S2 site and fusion peptides are activated. These activation/priming functions are performed by host enzymes namely furin and transmembrane serine protease 2 (TMPRSS2). While furin is involved in the cleavage at S1/S2 site of S protein, the activation of fusion peptides is carried out by transmembrane serine protease 2 (TMPRSS2) by cleaving at S2' site (figure 1). Thus, TMPRSS2 and furin host proteases play an important role in priming the S protein of the SARS-CoV-2 [11]. It is also important to note that the receptor binding mode of SARS-CoV-2 S/RBD with hACE2 is similar to that of earlier SARS-CoV/RBD-hACE2 complex. However, SARS-CoV-2 RBD forms more atomic interaction with hACE2

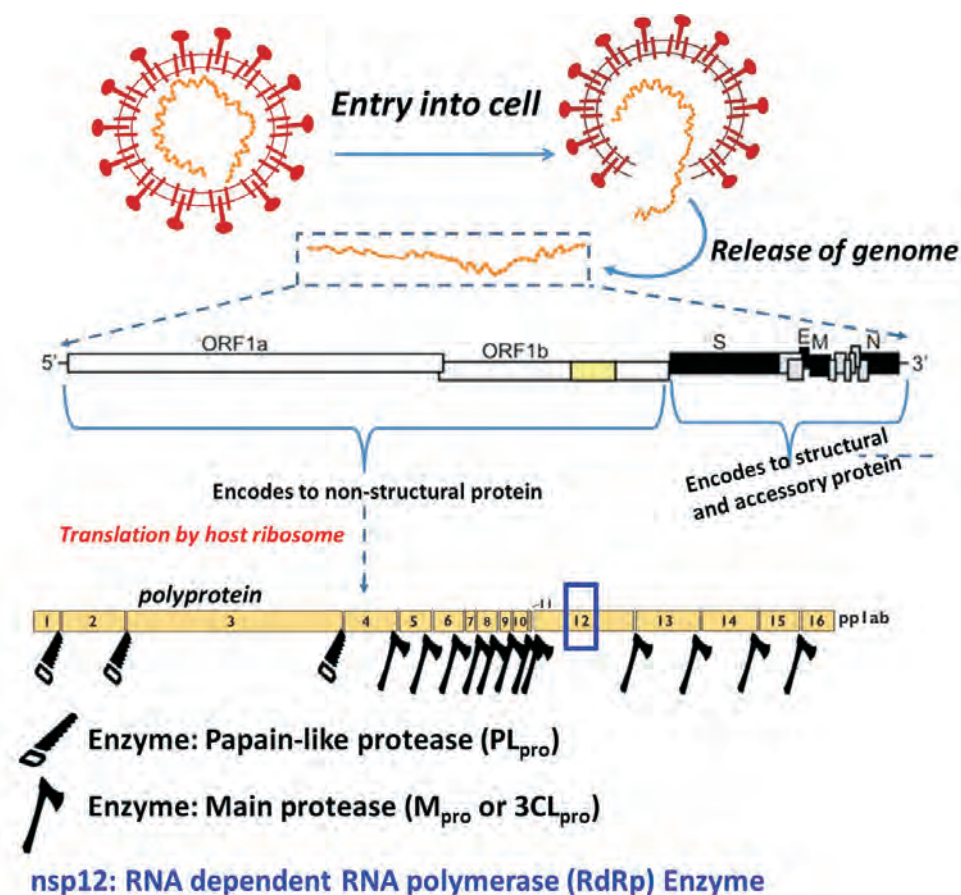


Fig. 2: Enzymes doing cleavage job to generate functional proteins essential for viral replication and assembly.

than SARS-CoV RBD as inferred from structural studies carried out by Wrapp et al and Wang et al [12, 13].

Since binding of the S protein with hACE2 marks the beginning of viral infection which is well assisted by the furin and TMPRSS2 host enzymes, blocking the binding between S protein and hACE2 is the key strategy for therapeutics and vaccine development. Neutralizing antibodies are increasingly recognized as potential options to primarily target trimeric S protein [14] while there are some small drugs such as chloroquine, arbidol, etc., [15, 16] and peptide binders [17] which are effective in

inhibiting the entry of virus. Moreover, there are phytochemicals like flavonoids and non-flavonoids which are effective in inhibiting the interaction between S protein and hACE2, owing to their high binding affinity towards S protein [18].

Enzymes facilitating protein cleavage, virus replication and assembly in host cell

Upon cell entry, viral RNA attaches to the host ribosome to yield two polyproteins pp1a and pp1ab that are essential for the production of new mature virions. As mentioned previously, the proteolytic cleavage of these two polyproteins is carried out

by papain-like protease (PL_{pro}) and the main proteinase (M_{pro} or $3CL_{pro}$). The X-ray structures of both $3CL_{pro}$ (PDB ID: 6W63) and PL_{pro} (PDB ID: 6W9C) from SARS-CoV-2 (COVID-19) are shown in (Figure 3). PL_{pro} from SARS-CoV-2 and SARS-CoV, share about 83% sequence identity, with amino acid composition [9]. The multifunctional PL_{pro} crystallographic homotrimer has Cys–His–Asp catalytic triad in each monomer. The Zn ions help in connecting the three monomers. PL_{pro} domain has cysteine-protease that cleaves the replicase polyprotein at the N terminus of pp1a, releasing nsp1- nsp3 [9]. PL_{pro} is not

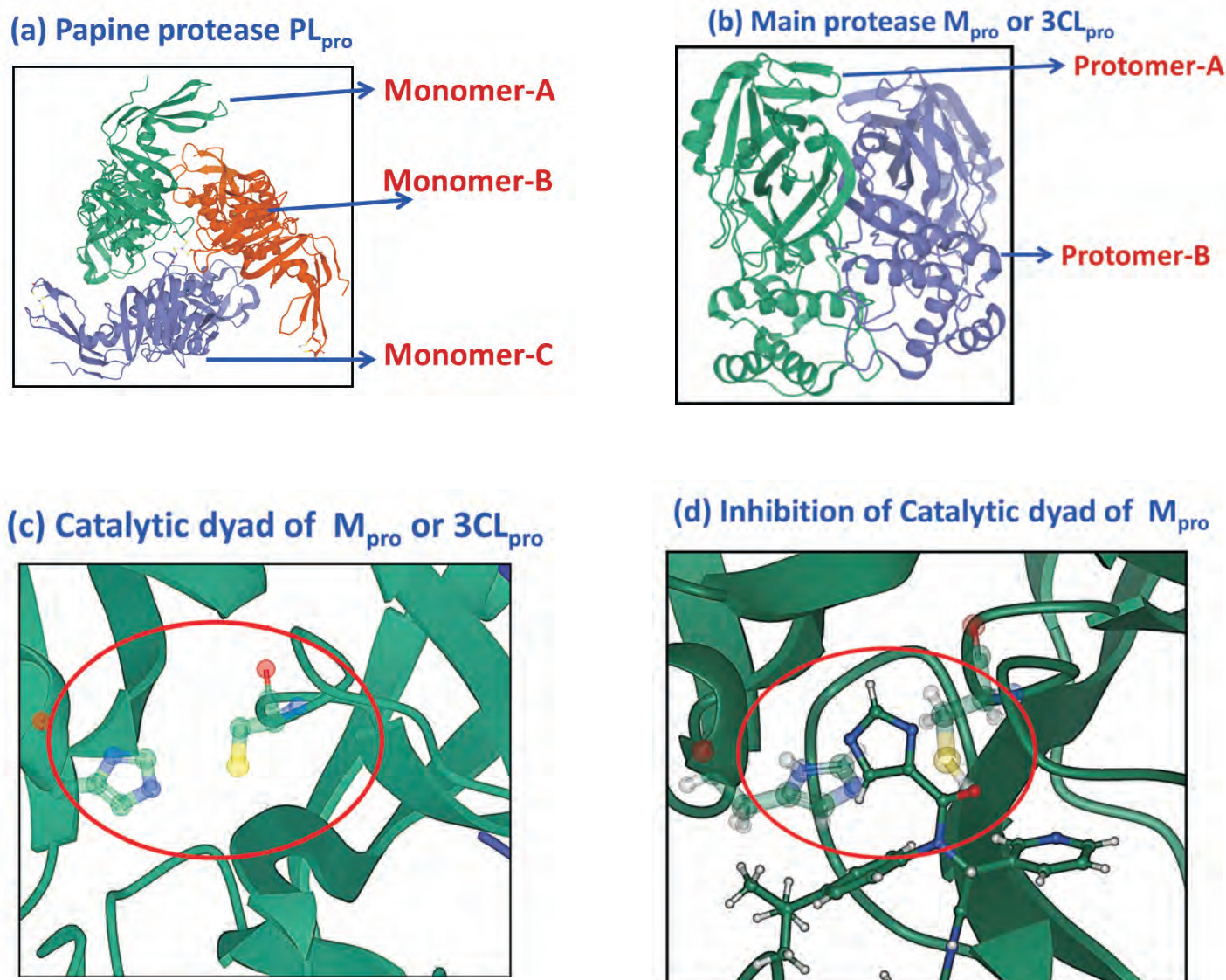


Fig. 3: Figure-3: (a) and (b) are the structure of enzyme PL_{pro} and M_{pro} . (c) depicts the catalytic dyad of M_{pro} and (d) shows interaction of drug with S atom of cysteine present in the catalytic dyad. Image is formulated at RCSB website

only is involved in cleaving the viral polyprotein, but it also is involved in removing cellular substrates like ubiquitin (Ub), termed deubiquitylation (DUB), and interferon-stimulated gene product 15 (ISG15) from host the cell proteins.

Like PL_{pro} homotrimer, the main protease 3CL_{pro} is a cysteine-protease but is active as a homodimer and utilizes a catalytic dyad (Cys-His) instead of a triad. Structure of M_{pro} deduced by Hilgenfeld et al [19] revealed that dimer form of M_{pro} is formed by linking of two protomers and each protomers has three domains. The catalytic dyad consisting of Cys145 and His41 residue is located in

a cleft as shown in Figure 3. Proteolysis of polyproteins by M_{pro} is achieved by the nucleophilic attack of by S atom of cysteine molecule at the catalytic site. Therefore the drugs which can be effective against the M_{pro} must contain an electrophilic centre which can engage the nucleophilic S atom thereby inhibiting the proteolysis of polyproteins and in turn viral replication. The Figure 3d shows inhibition of catalytic dyad by a representative drug molecule. Drugs which showed promise in impeding the function of M_{pro} are combination of lopinavir and ritonavir, carmofur, ketomamides, N3 inhibitors and phytochemicals like alkaloids,

terpenoids and polyphenolic compounds [19-24].

The 16nsp's generated from the proteolysis of polypeptide pp1a and pp1b finally form the viral replicase-transcriptase complex, which is responsible for the viral genome replication and subgenomic transcription. One of the key components/enzyme of this replicase-transcriptase complex is RNA dependent RNA polymerase (RdRp) enzyme, which is a domain of nsp12. RdRp is not a cleavage enzyme rather it is an enzyme that catalyzes the synthesis of RNA polymers. For SARS-CoV-2, RdRp enzyme

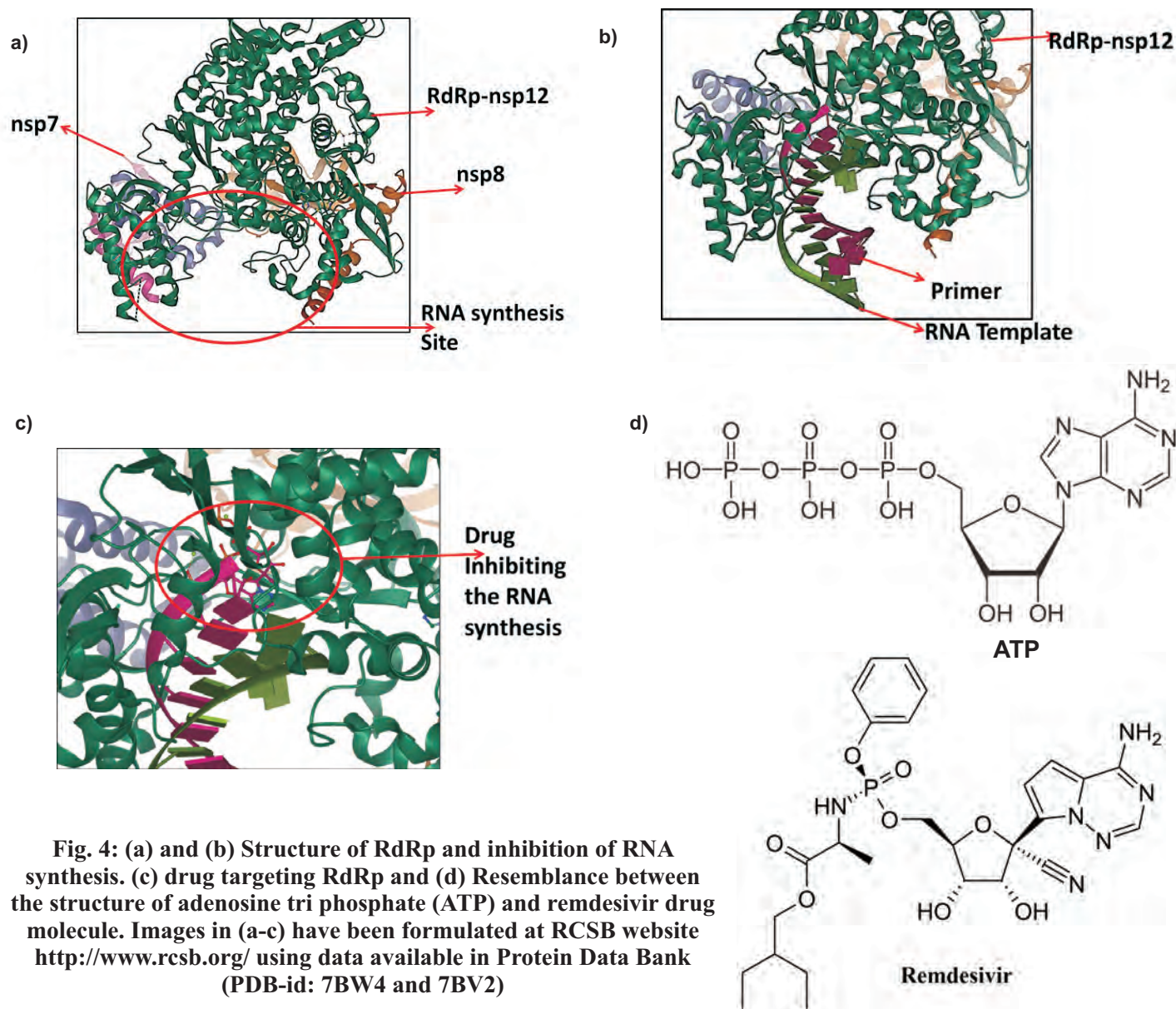


Fig. 4: (a) and (b) Structure of RdRp and inhibition of RNA synthesis. (c) drug targeting RdRp and (d) Resemblance between the structure of adenosine tri phosphate (ATP) and remdesivir drug molecule. Images in (a-c) have been formulated at RCSB website <http://www.rcsb.org/> using data available in Protein Data Bank (PDB-id: 7BW4 and 7BV2)

catalyzes the synthesis of viral RNA from RNA templates or building blocks and thus plays a central role in replication and transcription cycle of SARS-CoV-2 [25].

Structure of RdRp as deduced by Gao et. al. [25] revealed that it contains various sub-domains namely finger, palm and the thumb. (subdomain). The palm subdomain consists of catalytic cavity where polymerization of RNA building blocks takes place as shown in Figure-4. The nucleotide entry and exit path of RdRp are positively charged, which can be easily accessed by the solvent molecules. Proper functioning of RdRp enzyme demands cooperative efforts from its co-factors nsp7 and nsp 8, which help in boosting the catalytic activity of RdRp [26].

From the above discussion, it is clear that RdRp is the central component of SARS-CoV-2 replication and transcription machinery. This makes RdRp also an attractive target for antiviral drugs such as remdesivir, galidesivir, ribavarine, favipiravir, etc [26-27]. Structural studies of these promising drugs gave an insight that molecules which mimic the structure of RNA building blocks like adenosine, guanine, etc. are effective in impeding the activity of RdRp (Figure 4). By mimicking the RNS building block like adenosine triphosphate (ATP) it easily gets incorporated in nucleotide chain thus inhibiting the chain elongation process. In addition to the above drugs, there are phytochemicals like theaflavin was also found to be effective against RdRp [28].

Summary

The COVID-19 pandemic caused by highly transmissible SARS CoV-2 virus has strained the public health system besides seriously denting the prospects of global economic growth. This review outlines various important enzymes driving the (infection of SARS-CoV-2 infection either by

mediating in viral entry or assisting in replication and transcription process. Role of few salient enzyme like ACE2, Furin, TMPRSS2, PL_{pro}, M_{pro}, RdRp etc. has been discussed. These critical enzymes serve as attractive biological targets for drug development. The enzyme's structure, catalytic site and their role in infection has been discussed. This will indeed help in designing or repurposing the drug molecule which can be effective in blocking the entry or inhibit the replication of virus thereby terminating the infection. It is believed that review will provide the key learning points, and will serve as a primer for identifying novel therapeutic options.

Corresponding author and email:

Adish Tyagi (tyagia@barc.gov.in)

References

1. Gao, G. F. From "A"IV to "Z"IKV: Attacks from emerging and re-emerging pathogens. *Cell*, 2018, 172, 1157-1159.
2. Li, et. al. Early Transmission Dynamics in Wuhan, China, of Novel Coronavirus-Infected Pneumonia. *N Eng J Med*, 2020, <https://doi.org/10.1056/NEJMoa2001316>.
3. Wölfel, R., Corman, V. M., Guggemos, W., Seilmaier, M., Zange, S., Müller, M. A., Niemeyer, D., Jones, T. C., Vollmar, P., Rothe, C., Hoelscher, M., Bleicker, T., Brünink, S., Schneider, J., Ehmann, R., Zwirgmaier, K., Drosten C., Wendtner C. Virological assessment of hospitalized patients with COVID 2019. *Nature*, 2020 581, 465 469.
4. Harris, M., Bhatti, Y., Buckley, J., Sharma D. Fast and frugal innovations in response to the COVID 19 pandemic. *Nat Med*. 2 0 2 0 , <https://doi.org/10.1038/s4159102008891>.

5. Wu, D., Wu, T., Liu, Q., Yang, Z. The SARS-CoV-2 outbreak: what we know. *Int. J. Infect. Dis.* 2020, <https://doi.org/10.1016/j.ijid.2020.03.004>.
6. Katsnelson, A. What we know about the novel coronavirus's proteins. *CEN. ACS. ORG.* 2020, <https://cen.acs.org/biological-chemistry/infectious-disease/know-novel-coronaviruss-29-proteins/98/web/2020/04>.
7. Yan, R., Zhang, Y., Li, Y., Lu, X., Guo, Y., Zhou, Q. Structural basis for the recognition of SARS-CoV-2 by full-length human ACE2. *Science*, 2020, 367, 1444-1448.
8. Walls, A. C., Park, Y. J., Tortorici, M. A., Wall, A., McGuire, A. T., Velesler, D. Structure, Function, and Antigenicity of the SARSCoV-2 Spike Glycoprotein. *Cell*, 2020, 180, 281-292.
9. Ghosh, A. K., Brindisi, M., Shahabi, D., Chapman, M. E., Mesecar, A. D. Drug Development and Medicinal Chemistry Efforts toward SARS Coronavirus and Covid 19 Therapeutics. *ChemMedChem*, 2020, 15, 907-932.
10. Tang, T., Bidon, M., Jaimes, J. A., Whittaker, G. R., Daniel, S. Coronavirus membrane fusion mechanism offers a potential target for antiviral development. *Antivir. Res.* 2020, 178, 104792.
11. Hoffmann, M., Weber, H. K., Schroeder, S., Kruger, N., Herrler, T., Erichsem S., Schiergens T. S., Herrler, G., Wu, N. H., Nitsche, A., Muller, M. A., Drosten C., Pohlmann, S. SARS CoV 2 Cell Entry Depends on ACE2 and TMPRSS2 and Is Blocked by a Clinically Proven Protease Inhibitor. *Cell*, 2020, 181, 271 280.e8.
12. Wrapp, D., Wang, N., Corbett, K.

- S., Goldsmith, J. A., Hsieh, C. L., Abiona, O., Graham, B. S., McLellan, J. S. (2020) Cryo EM structure of the 2019 nCoV spike in the prefusion conformation. *Science*, 2020, 6483, 1260-1263.
13. Wang, Qi. h., Zhang Y., Wu Lili, Niu, Sheng, Song, C., Zhang, Z., Lu, G., Qiao, C., Hu, Y., Yuen, K. Y., Wang, Q., Zhou, H., Yan, J., Qi, J. (2020) Structural and Functional Basis of SARS CoV 2 Entry by Using Human ACE2. *Cell*, 2020, 181, 894-904.
14. Wang, C. et. al. A human monoclonal antibody blocking SARS-CoV-2 infection. *Nat. Commun.* 2020, <https://doi.org/10.1038/s41467-020-16256-y>.
15. Hu, T. Y., Frieman, M., Wolfram, J. Insights from nanomedicine into chloroquine efficacy against COVID 19. *Nat. Nanotech.* 2020, 15, 247-249.
16. Vankadari N. Arbidol: A potential antiviral drug for the treatment of SARS CoV 2 by blocking trimerization of the spike glycoprotein. *Int. J. Antimicrob. Agents*, 2020, 105998 DOI: <https://doi.org/10.1016/j.ijantimicag.2020.105998>.
17. Zhang, G., Pomplun, S., Loftis, A. R., Loas, A. and Pentelute, B. L. The first in class peptide binder to the SARS CoV 2 spike protein, *bioRxiv* 2020, doi: <https://doi.org/10.1101/2020.03.19.999318>.
18. Rane, J. S., Chatterjee, A., Kumar A., and Ray, S. (2020) Targeting SARS CoV 2 spike protein of COVID 19 with naturally occurring Phytochemicals: an In silico study for drug development. *ChemRxiv*, 2020, DOI: <https://doi.org/10.26434/chemrxiv.12094203.v1>.
19. Zhang, L., Lin, D., Sun, X., Curth, U., Drosten, C., Sauerhering, L., Becker, S., Rox. K., Hilgenfeld, R. Crystal structure of SARS CoV 2 main protease provides a basis for design of improved ketoamide inhibitors. *Science*, 2020 368, 409-412.
20. Cao, B. A Trial of Lopinavir-Ritonavir in Adults Hospitalized with Severe Covid-19. *N Engl J Med* 2020, 382, 1787-1799
21. Jin, Z., Zhao, Y., Sun, Y., Zhang, B., Wang, H, Wu, Y., Zhu, Y., Zhu, C., Hu, T., Du, X., Duan, Y., Yu, J., Yang, X., Yang, X., Yang, K., Liu 6, X., Guddat, L.W., Xiao, G., Zhang, L., Rao, H.Y.Z. Structural basis for the inhibition of SARS CoV 2 main protease by antineoplastic drug carmofur, *Nat. Struct. Mol. Bio.*, 2020, DOI: <https://doi.org/10.1038/s41594-020-0440-6>.
22. Jin, Z., Du, X., Xu, Y., Deng, Y., Liu, M., Zhao, Y., Zhang, B., Li, X., Zhang, L., Peng, C., Duan, Y., Yu, J., Wang, L., Yang, K., Liu, F., Jiang, R., Yang, X., You, T., Liu, X., Yang, X., Bai, F., Liu, H., Liu, X., Guddat, L.W., Xu, W., Xiao, G., Qin, C., Shi, Z., Jiang, H., Rao Z., & Yang, H. (2020) Structure of Mpro from SARS CoV 2 and discovery of its inhibitors. *Nature*, DOI: <https://doi.org/10.1038/s41586-020-2223-y>.
23. Gyebi, G. A., Ogunro, O. B., Adegunloye, A. P., Ogunyemi O. M., & Afolabi, S. O. Potential Inhibitors of Coronavirus 3 Chymotrypsin Like Protease (3CLpro): An in silico screening of Alkaloids and Terpenoids from African medicinal plants. *J. Biomol. Str. Dyn.* 2020, DOI: <https://doi.org/10.1080/07391102.2020.1764868>.
24. Qamar, M. T., Alqahtani, S. M., Alamri, M. A., Chen, L. L. Structural basis of SARS CoV 2 3CLpro and anti COVID 19 drug discovery from medicinal plants. *J. Pharm. Anal.* 2020, DOI: <https://doi.org/10.1016/j.jpha.2020.03.009>.
25. Gao, Y. et. al. Structure of the RNA-dependent RNA polymerase from COVID-19 virus. *Science*, 2020, 368, 779-782.
26. Zhang, W., Stephan, P., Thériault, J. F., Wang, R., Lin, S. X. Novel Coronavirus Polymerase and Nucleotidyltransferase Structures: Potential to Target New Outbreaks. *J. Phys. Chem. Lett.*, 2020, DOI: [10.1021/acs.jpcclett.0c00571](https://doi.org/10.1021/acs.jpcclett.0c00571).
27. Yin, et. al. Structural basis for inhibition of the RNA-dependent RNA polymerase from SARS-CoV-2 by remdesivir. *Science*, 2020, DOI: [10.1126/science.abc1560](https://doi.org/10.1126/science.abc1560).
28. Lung, J., Lin, Y. S., Yang, Y. H., Chou, Y. L., Shu, L. H., Cheng, Y. C., Liu, H. T., Wu, C. Y. The potential chemical structure of anti SARS CoV 2 RNA dependent RNA polymerase. *J Med Virol.*, 2020, 92, 692-697.



Central Complex BARC

Edited & Published by:
Scientific Information Resource Division
Bhabha Atomic Research Centre, Trombay, Mumbai 400 085, India
BARC Newsletter is also available at URL:<http://www.barc.gov.in>